Extended Alkenyl and Alkynyl Benzotriazoles with enhanced Two-Photon Absorption properties as a promising alternative to Benzothiadiazoles

Iván Torres-Moya,[a,+] Carlos Benítez-Martin,[b,c,+] Beatriz Donoso,[a] Carlos Tardío,[a] Raúl Martín,[a] José R. Carrillo,[a] Ángel Díaz-Ortiz,[a] Francisco Nájera,*[b,c] Pilar Prieto,*[a] and Ezequiel Pérez-Inestrosa*[b,c]

Abstract: A series of D-π-A-π-D benzoazole dyes with 2*H*-benzo[*d*][1,2,3]triazole (BTz) or Benzo[*c*][1,2,5]benzothiadiazole (BTD) cores have been prepared and their photophysical properties characterized. The properties of these compounds display remarkable differences mainly managed by the electron-donor substituent. The dyes with the best properties have visible-light absorption over 400 nm, large Stokes shifts in the range of *ca.* 3500–6400 cm^{-1} and good fluorescence emission with quantum yields of up to 0.78. Their two-photon absorption (TPA) properties were also studied in order to stablish a relationship between structure and properties in the different compounds synthesized. They provided cross-sections up to 1500 GM, with predominance of the $S_2 \leftarrow S_0$ transition and a high charge-transfer character. Time-dependent (TD)-DFT calculations supported the experimental results.

Introduction

Due to their excellent photophysical properties the benzoazoles derivatives have aroused great interest in fluorescence-related applications in recent years. Among them, the 1,2,5-benzothiadiazoles (BTD) have been the most studied due to their excellent fluorescence quantum yields and profitable Stokes shifts. The blend of their photophysical properties with a high synthetic versatility, appoints BTD as the protagonist of many usages. Some of the numerous fields in which they have been applied are photocatalysis,[1] bioimaging[2] or even in designing solar cells.[3] The iminic bonds in their structure bestow a prominent electron-acceptor character to the BTD units extending their use to fluorescent scaffolds, especially when intramolecular charge transfer (ICT) is demanded.

In addition to BTD,[4] our research in the recent years has also focused on 2*H*-benzo[*d*][1,2,3]triazole (BTz) as other benzoazole derivative. BTz is an interesting option to be considered since this moiety accomplishes excellent photophysical properties.[5,6] Despite the fact that BTz is a less accepting core than BTD, this unit allows better functionality. It is possible not only to introduce groups in positions 4 and 7, but also to functionalize the nitrogen 2. This affords to modulate the acceptor character and increase the solubility of the structures. BTz and its derivatives are known as multitask unit with a wide application in some fields. They are employed as antifreeze and corrosion-inhibiting agent in several systems,[7] and as copolymer in donor-acceptor (D-A) polymers with application in solar cells.[8–11] In the last years our research group has also described their applications as optical waveguide,[6] semiconductors in OFETs,[12] organogel[13] as soon well as bioimaging.[14]

Since its prediction by Göppert-Mayer,[15] TPA spectroscopy has emerged as an attractive tool to further study basic properties of materials and matter-light interactions. Over the last years, the interest in materials which exhibit TPA has been widely increased due to the development of applications such as 2D microfabrication,[16] optical data storage[17,18] and two-photon induced fluorescence (TPIF) imaging,[19] among others.

In order to avoid unnecessary synthesis and reduce the environmental impact of Chemistry, avoiding the trial and error method as far as possible should be a paramount objective. TPA properties are close related with the molecular architecture, making essential the identification of structure-property relationships. The best known approaches are mainly based on combining different electron feature moieties to constitute a dipolar donor-acceptor structure, which is usually assembled by a π-conjugate system. Thus, ICT character is a key feature for large TPA cross-sections. Even if any possibility of combination between different electron-behavior units can be achieved, the best results are obtained with centrosymmetric quadrupolar π-conjugated dyes with terminal donor or acceptor substitution and with symmetrical designs displaying donor groups in the periphery of the molecule, i.e., D-π-D or D-π-A-π-D patterns.[20–25]

Although the BTD core has been used as electron-withdrawing core in molecules with TPA character,[26–28] we have not found any example using the BTz unit for this purpose. With this aim, in this work we have studied three different conjugated benzoazole derivatives families (Figure 1), such as the previously synthesized alkynyl derivatives of BTD[4] and BTz,[5,6,12,13] and a new family of alkenyl BTz derivatives. The objective of this study is to attempt to deepen the relationship between structure and TPA properties

[a] Dr. I. Torres-Moya, B. Donoso, C. Tardío, R. Martín, Dr. J.R. Carrillo, Prof. Dr. A. Díaz-Ortiz and Dr. P. Prieto
Department of Organic, Inorganic Chemistry and Biochemistry
Faculty of Chemical and Technologies Sciences-IRICA
13071, Ciudad Real (Spain)
E-mail: Mariapilar.Prieto@uclm.es

[b] C. Benitez-Martin, Dr. F. Najera and Prof. Dr. E. Perez-Inestrosa
Universidad de Málaga-IBIMA, Departamento de Química Orgánica.
Campus de Teatinos s/n, 29071-Málaga, Spain.
E-mail: najera@uma.es; inestrosa@uma.es

[c] C. Benitez-Martin, Dr. F. Najera and Prof. Dr. E. Perez-Inestrosa
Centro Andaluz de Nanomedicina y Biotecnología-BIONAND.
Parque Tecnológico de Andalucía, c/Severo Ochoa, 35, 29590 Campanillas, Málaga, Spain.
E-mail: najera@uma.es; inestrosa@uma.es

[+] These authors contributed equally to this work.

Supporting information for this article is given via a link at the end of the document.

particularized to these types of benzoazole structures and to present the BTz as a new building block for TP chromophores.

Results and Discussion

In our group we have worked in depth in recent years on the synthesis and applications of alkynyl benzoazoles. Thus, we have described alkynyl- 2*H*-benzo[*d*][1,2,3]triazole derivatives (**1**) (Figure 1) with a wide variety of applications, as indicated above. These compounds were synthesized by means of a Sonogashira C-C cross-coupling reaction under microwave irradiation.[6,12]
Following this same methodology we have also described alkynyl-benzo[*c*][1,2,5]thiadiazole (**3**) (Figure 1) with application as optical waveguides and Amplified Spontaneous Emission (ASE).[4]
Due to the enormous potential of these compounds, now we approach their study as TP chromophores. Since there are no studies in the literature about the TPA properties of benzotriazoles and with the aim of studying this property in depth in this type of compounds, in this work we have also synthesized alkenylbenzotriazoles derivatives (**2**) in order to compare the influence of the π-spacer (Figure 1).

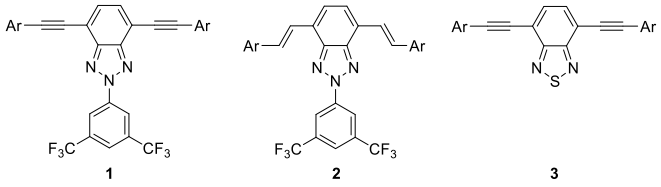

Figure 1. Different conjugated benzoazole derivatives studied.

Design and synthesis

Alkenylbenzotriazole derivatives **2a**, **2c** and **2d** were obtained through a Heck C-C cross-coupling reaction between the dibromobenzotriazole **4** and the arylalkenes **5a**, **5c** and **5d** in moderate to good yields (41-86%) (Scheme 1).
The reactions were performed in an inert atmosphere using $Pd(OAc)_2$ as the catalyst, with NaOAc and TBAB in DMF at 100 °C for 24 h.[29] Arylalkene **5a**, (styrene), is commercial, although it was purified by distillation prior to its use, while **5c** and **5d** were prepared by means of a Wittig reaction from the corresponding aldehyde and Ph_3PMeBr.[30]
Derivative **2b** could not be synthesized employing this synthetic method, but it was obtained in good yield (71%) by partial reduction of **1b** (Scheme 1). This palladium-catalyzed [$PdCl_2$(dppf)/dppf] semi-hydrogenation employs $HSiEt_3$ as the reductant, and $CuSO_4$ to assure a *trans* stereoselectivity of the double bond C=C.[31]
All the compounds were purified by silica gel column chromatography using hexanes/ethyl acetate as the eluent and gave satisfactory analytical mass spectroscopy (MS) and spectroscopic (NMR) data (see Supporting Information).

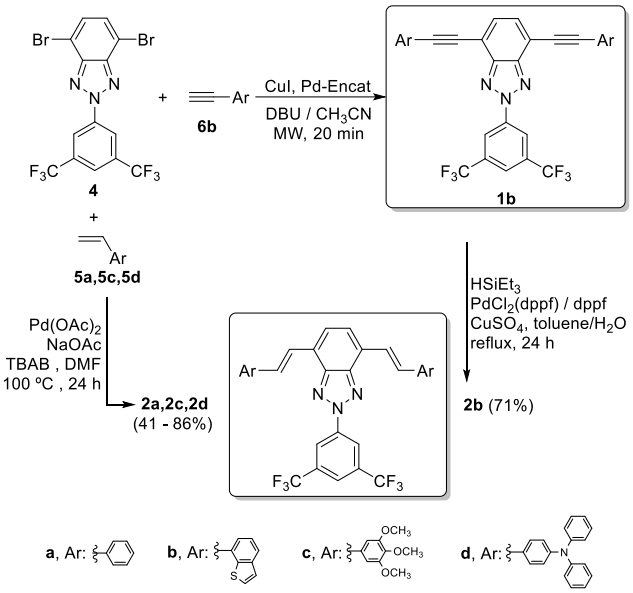

Scheme 1. Synthetic procedures for the preparation of derivatives **2**.

Photophysical properties

The analysis of the photophysical data of these compounds, under one-photon (OP) conditions, provides clear trends in their properties (Table 1). In absorption spectra, the longest-wavelength bands cover the region from blue to cyan. Their maxima are located between 373 nm until 490 nm and are associated to $S_1 \leftarrow S_0$ transitions. The placement of absorption bands is related with the push-pull character of the dyes. They are gradually red-shifted when the electron-donating character of the peripheral groups are improved, as can be appreciated in the spectra of the compounds **2a-d** (Figure 2, see the Supporting Information for the spectra of **1a-d** and **3a-d,** Figures S1-S2). Thus, phenyl derivatives (series **a**), considered as the starting pattern, have their absorption bands shifted to blue as a consequence of having the weakest electron-donor group. Moreover, dyes with the benzothiophene (series **b**) and the trimethoxybenzene moieties (series **c**) achieve similar displacements in absorption terms. If comparing to series **a**, their bands move to less energetic wavelengths and in almost equal extent. Compounds containing the triphenylamine group (series **d**), the strongest electron-donor moiety in these derivatives, display the most bathochromically shifted absorption.

Table 1. Photophysical data OP and TP of the dyes in chloroform (10^{-5}M, air-equilibrated solutions).

Compound	λ_{abs}^{OP} (nm) [ε, $M^{-1}cm^{-1}$][a]	λ_{fluo}^{OP} (nm) [b]	Φ_{fluo} [c]	Δν (cm^{-1})[d]	λ_{exc}^{TP} (nm)[e]	λ_{fluo}^{TP} (nm) [f]	σ (GM)[g]	Φσ (GM)
1a	373 [15393]	454	0.78	4783	710	460	9	7
1b	411 [34990][h]	514[h]	0.78[h]	4876	750	505	33	26
1c	412 [11061][h]	529[h]	0.71[h]	5368	730	535	104	74
1d	464 [31980][h]	572[h]	0.32[h]	4069	840	580	1510	483
2a	429 [12913]	521	0.40	4116	720	520	39	16
2b	448 [15362]	531	0.41	3489	740	535	125	51
2c	446 [7517]	555	0.60	4404	740	565	131	79
2d	490 [12668]	603	0.20	3824	830	610	790	158
3a	413 [34169]	507	0.68	4489	710	520	29	20
3b	430 [58450]	518	0.53	3951	750	520	129	68
3c	428 [15500][i]	590[i]	0.49[i]	6415	730	580	88	43
3d[j]	484 [41528]	624	0.26	4636	830	625	545	142

[a] Longest-wavelength absorption maximum, in square brackets the corresponding molar absorption coefficient. [b] Fluorescence emission maximum. [c] Fluorescence emission quantum yield. [d] The Stokes shift as the difference between the maxima of the wavenumber converted absorption and emission spectra. [e] Wavelength corresponding to the highest cross section. [f] TP emission maxima, (the spectra were measured using a dynamic 30 nm wide emission detection window moving in 20 steps between 380 and 700 nm). [g] TPA cross sections were measured in the range of 700-1000 nm. [h] OP absorption and emission obtained from ref. [6]. [i] OP absorption and emission obtained from ref. [4]. [j] The TP-properties of this compound have been previously evaluated by open aperture *Z*-scan technique (λ_{abs}^{OP} (CH_2Cl_2) = 484 nm, λ_{fluo}^{OP} (CH_2Cl_2) = 663 nm, Φ_{fluo} (CH_2Cl_2) = 0.19, λ_{exc}^{TP} (toluene) = 800 nm; λ_{fluo}^{TP} (toluene) = 586 nm, σ = 200 GM measured in a 2.0 x 10^{-3} M toluene solution. Differences in the determined cross-section values can be associated to the concentration of the samples and the used methodologies in their determination); ref. [27].

The displacement to longer wavelengths of the absorption bands in compounds **2a-d**, compared to the **1a-d** ones, is not only affected by the push-pull phenomena. The level of π-conjugation along the structure is equally important. Stronger conjugation favored by the presence of vinylene- instead of ethynylene-bridge eases the electronic movement and promotes the red-shifting of these bands. The introduction of BTD in the alkynyl-derivatives (compounds **3a-d**) is also relevant. The slight increment in the electron-acceptor character of the chromophore-core also moves the absorption bands to longer wavelengths compared to **1a-d**, but in milder extension compared to vinylene-compounds **2a-d**.

Fluorescence bands of these dyes are located in a wide spectral region comprised between 450 nm and 625 nm (Table 1), considerably far from absorption ones, and displaying Stokes shifts up to 6415 cm^{-1}. These emission maxima are also related to the push-pull effects and the π-conjugation level. Contrasting with the absorption maxima, trimethoxybenzene moiety (series **c**) attains a larger shift in the emission in comparison to benzothiophene group (series **b**). In the same manner, when the donor feature is enhanced, the emission bands notably change if compared to phenyl derivatives (series **a**), yielding the most red-shifted bands when the triphenylamino group is incorporated in the scaffold as donor group (series **d**).

In general, these compounds display moderate to high fluorescence quantum yields (Φ_{fluo}), from 0.20 until 0.78 (Table 1). Dyes **1a-d** and **3a-d** attain higher fluorescence quantum yields in comparison to **2a-d**. This issue is a consequence of the lack of photo-isomerization in the alkynyl-derivatives. Interesting to highlight in the properties of these compounds are their high Stokes shifts in parallel to their good fluorescent quantum yields. This junction is not always available in other fluorescent scaffolds such as BODIPYs or cyanines.[32]

Solvatofluorochromic properties

As a result of associating different electron-behavior groups, it is expected that the photophysical properties of derivatives **2** will be governed by an ICT character, as well as it is reported for derivatives **1** and **3**.[4,6,27] Absorption and emission of compound **2d** were studied in different solvents to further evaluate the influence of the polarity in its photophysical properties, as detailed in the Supporting Information (Table S1). Regarding UV/vis absorption maxima, which are about 485 nm, slight differences are observed. Notwithstanding, a notable displacement is appreciated in emission bands as the polarity increases (Figure 3).

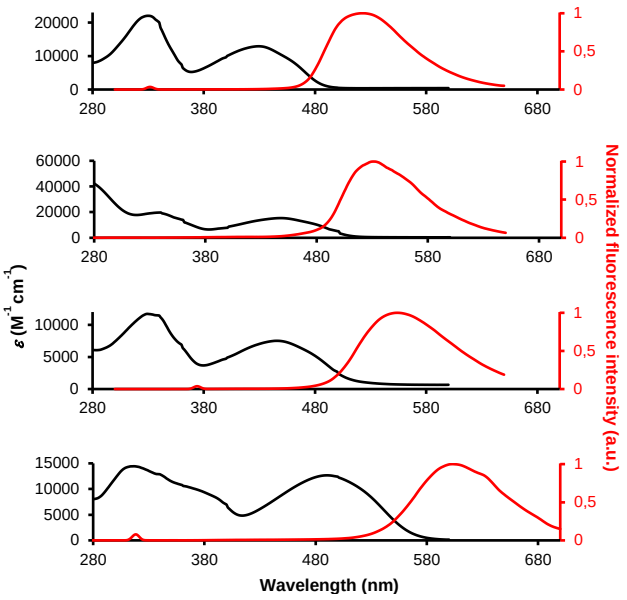

Figure 2. Absorption (black lines) and emission spectra (red lines) of family **2** (from up to bottom: **2a**, **2b**, **2c** and **2d**). The fluorescence spectra were obtained by excitation at the long-wavelength of maximum absorbance.

The fluorescence spectra of compound **2d** are characterized by broad and structureless bands. Emission maxima display positive solvathrochromic effects, displacing from 560 nm in *n*-hexane to 643 nm in dimethylformamide (DMF).

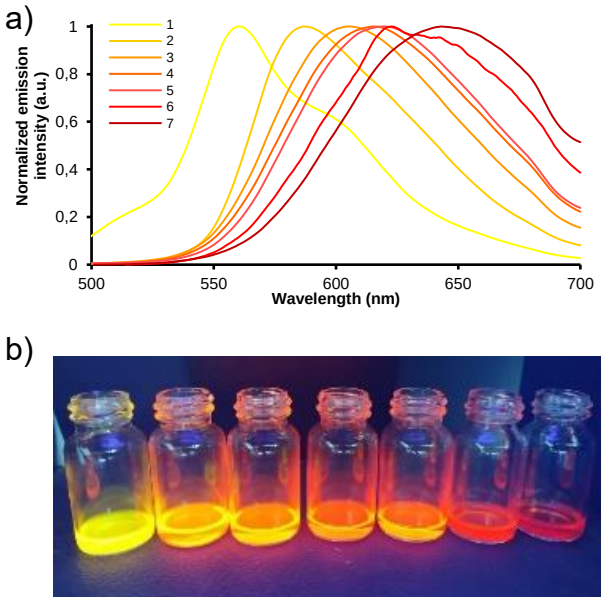

Figure 3: a) Normalized fluorescence spectra of **2d** in different solvents (from left to right): 1) *n*-hexane, 2) toluene, 3) chloroform, 4) THF, 5) dichloromethane, 6) acetone and 7) DMF. b) Solutions of **2d** in the mentioned above solvents at 10^{-5} M, excited under 365 nm light.

This switch of 83 nm when increasing the polarity, clearly adjusts to the ICT character of the emission band. Furthermore, the Lippert-Mataga plot[33–35] of the Stokes shift versus the orientation polarizability (Δf) showed an excellent correlation, yielding a difference in dipole moment between excited and ground state of 15.41 D for compound **2d** (Figure S3).

Two-photon absoption properties

The TPA properties of these compounds were fully investigated by the method of two-photon-induced fluorescence (TPIF),[36] in a range comprised between 700 nm and 1000 nm. The data are summarized in Table 1 and the full TP excitation and TPIF emission spectra can be found in Figure 4a and in Figures S4-S14.

Examining the determined cross-section values (Table 1), the chromophores with the best electron-donor substituent accomplish the greatest values, as high as 1510 GM at 840 nm for **1d**, 790 GM at 830 nm for **2d** and 545 GM at 830 nm for **3d** (Figure 4b). Conversely, compounds of series **a**, address the lowest values regardless of the core considered (Figure S15).

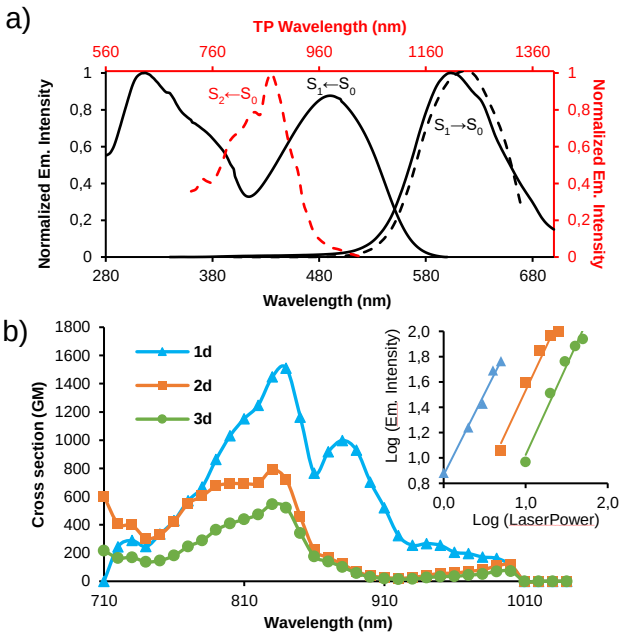

Figure 4. a) Absorption and emission spectra of compound **2d** under OP regime (bold lines). Excitation (red dashed line) and emission spectra (dashed black line) of **2d** under TP conditions. Involved electronic states are indicated in each case. The same electronic states are implicated in fluorescence in both cases. b). Cross-section of compounds **1d, 2d, 3d**. The inset shows the double-logarithmic plot of the emission maximum intensity versus laser power for compounds above mentioned.

About the other compounds, similar features are appreciated. Generally, benzothiophene moiety (**2b** and **3b**) renders better results than trimethoxyphenyl group (**2c** and **3c**), excepting for dyes **1b** and **1c**, which bear the opposite behavior (Figures S16-

S17). The change in the π-bridge from ethynylene to vinylene (compounds **1a-c** *versus* **2a-c**) causes an enhancement in the conjugation grade and improves their TPA. Surprisingly, the cross-section of compound **1d** is higher than **2d** ones. In this case, the movement of the electrons is not the only key factor to be considered, the steric congestion is also an important issue. The presence of bulky groups, such as BTz-core and the triphenylamino moiety, favors the movement of electrons when ethynylene-bridge is incorporated avoiding the twist out of conjugation.[37]

The change in the core of these dyes affords similar or better cross-sections for the BTz-derivatives in relation to BTD ones. In the former, the presence of the 3,5-bis(trifluoromethyl)phenyl group in the position 2 of the core, enhances its electron-withdrawing feature under two-photon conditions.

These compounds exhibit remarkable brightness values up to 483 GM (Table 1). Although fluorescence quantum yields are weaker in **2a-d**, the improved TPA properties of this family assures high brightness values in these compounds.

Similar maxima and band shapes are obtained for the fluorescence emission of these compounds regardless of the nature of the excitation process. However, the OP absorption and TP excitation wavelengths do not match as it was expected. It is well known that some TP chromophores perform a $S_2 \leftarrow S_0$ transition instead of the classical $S_1 \leftarrow S_0$, joining higher electronic states (Figure 4a and Figures S4-S14).[38,39]

DFT calculations

Density-functional theory (DFT) and time-dependent density-functional theory (TD-DFT) were performed for all compounds to obtain additional insight into the photophysics of the investigated dyes. Therefore, the Coulomb-attenuate CAM-B3LYP functional[40] and the 6-31G(d) basis set[41] were employed for the estimation of geometrical parameters and the 6-311+G(2d,p) basis set was used to determine absorption and emission energies. The solvent medium, chloroform, was included by the use of polarization continuum model (PCM).[42]

The trends in the photophysical properties are well reproduced for all compounds. The natural transition orbital (NTO) analysis[43] for the lowest energy transitions ($S_1 \leftarrow S_0$) of these compounds are shown in Figure 5 and Figures S18-S29. Primarily centered in the donor groups, the NTO holes are also located through the π-bridge and a minimal part of the core. Albeit, the NTO electrons are fully centered along the core of the molecules. This pronounced change in the electronic density is commonly related with an ICT process and it agrees with the experimental data for these dyes.[4,6,27] Going further, $S_1 \leftarrow S_0$ transition is mainly populated by the HOMO and the LUMO frontier orbitals. As expected, the same orbitals are implicated in the emission process (Table 2).

In consequence, the maxima of both absorption and emission spectra attend to the trend that is conducted by the calculated HOMO-LUMO energy band gap. In this manner, compounds of series **a** hold the largest band gap energies as consequence of a less prominent ICT. Just the opposite behavior is observed for the series **d**, which display improved ICT as well as lower band gap energies (Table 2).

The TPA properties were calculated at the CAM-B3LYP/6-31G level. In all cases, the theoretical results indicate that the active transition under TP regime is the $S_2 \leftarrow S_0$ instead of $S_1 \leftarrow S_0$. This bearing is in consonance with the experimental results (Figure 4a and Figures S4-S14) and the predicted OPA and TPA spectra (Figures S30-S41). The NTO analysis relative to the $S_2 \leftarrow S_0$ transition indicates that the ability as TP chromophore is closely related to the change in the distribution of the electronic density.

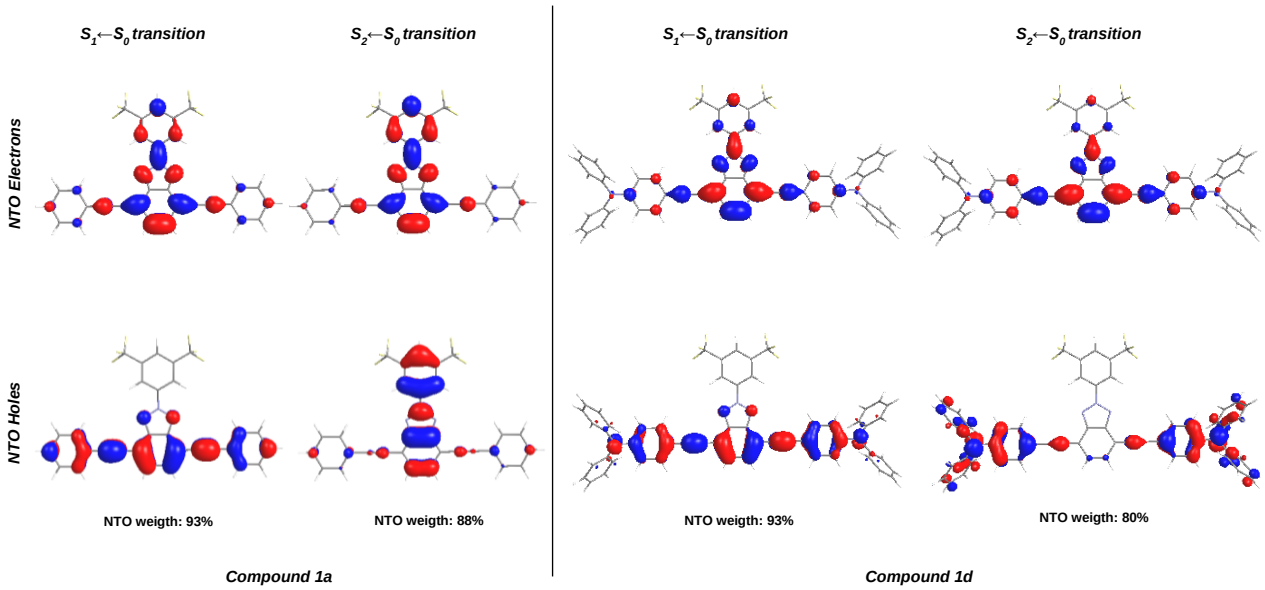

Figure 5. NTOs for $S_1 \leftarrow S_0$ and $S_2 \leftarrow S_0$ transitions in compounds **1a** and **1d**.

In Figure 5 the $S_2 \leftarrow S_0$ transitions for compounds **1a** and **1d** are indicated, which address the lowest and the highest experimental cross-section values respectively. While in compound **1a**, the electron density is always distributed over the acceptor unit regardless if considering both NTO hole or NTO electron, in compound **1d**, the electron density drastically moves from the donor groups in the NTO hole to the acceptor core in the NTO electron. This behavior nicely confirms the ICT trend in this transition (Figures S18-S29).

Conclusions

The photophysical properties of a series of D-π-A-π-D benzoazole dyes, with BTz or BTD as acceptor cores, were studied under OP and TP conditions. Emission maxima in the BTz-dyes are efficiently tuned through modulation of the donor groups and the π-bridge. These compounds allow to cover a wide range of the UV-vis region (from 454 nm to 603 nm) and highlight for combining large Stokes shifts and good quantum yields.
Under two-photon conditions, these dyes have high brightness and cross-sections up to 1510 GM with triphenylamino as donor group. The presence of the bis(trifluoromethyl)phenyl group in the BTz-core gives an improved electron-withdrawing character to the acceptor unit. Hence, BTz-dyes display large cross-sections values even higher than BTD ones. Contrary to OP absorption, the TP excitation is controlled by $S_2 \leftarrow S_0$ transition, displaying a charge-transfer character and agreeing with the theoretical studies.

Experimental Section

General Methods: All reagents were used as purchased unless otherwise stated. Reactions with air-sensitive materials were carried out under an argon atmosphere. Compounds **1a-d**, **3a**, **3c** and **3d** have been prepared as reported before.[4–6,12,13] Flash chromatography was perfomed using silica gel (Merck, Kieselgel 60, 230–240 mesh or Scharlau 60, 230–240 mesh). Analytical thin layer chromatography (TLC) was performed using aluminium-coated Merck Kieselgel 60 F254 plates. ^{1}H-NMR and ^{13}C-NMR spectra were recorded on a Varian Unity 500 (^{1}H: 500 MHz; ^{13}C: 125 MHz) spectrometer at 298 K using partially deuterated solvents as internal standards. Coupling constants (*J*) are denoted in Hz and chemical shifts (δ) in ppm. Multiplicities are denoted as: s = singlet, d = doublet, t = triplet, m = multiplet, br = broad.

Table 2. Calculated electronic and photophysical data for the dyes **1a-d**, **2a-d** and **3a-d**.[a]

Compound	Absorption				Emission				
	f[b]	Dominant Component (%)[c]	$E_{max\ calc.}$ (eV)[d]	$E_{max\ exp.}$ (eV)[d]	f[b]	Dominant Component (%)[c]	$E_{max\ calc.}$ (eV)[d]	$E_{max\ exp.}$ (eV)[d]	$\Delta E_{HOMO-LUMO}$ (eV)[e]
1a	1.436	LUMO←HOMO (93)	3.13	3.32	1.416	LUMO→HOMO (96)	2.50	2.73	5.30
1b	1.481	LUMO←HOMO (89)	3.03	3.02	1.510	LUMO→HOMO (94)	2.41	2.41	5.29
1c	1.586	LUMO←HOMO (92)	3.08	3.01	1.576	LUMO→HOMO (95)	2.44	2.34	5.20
1d	2.140	LUMO←HOMO (78)	2.82	2.67	2.065	LUMO→HOMO (89)	2.22	2.17	4.64
2a	1.334	LUMO←HOMO (95)	2.88	3.01	1.322	LUMO→HOMO (97)	2.20	2.38	5.04
2b	1.426	LUMO←HOMO (92)	2.84	2.77	1.440	LUMO→HOMO (96)	2.15	2.33	4.95
2c	1.428	LUMO←HOMO (92)	2.82	2.78	1.411	LUMO→HOMO (96)	2.13	2.23	4.89
2d	1.944	LUMO←HOMO (82)	2.63	2.53	1.881	LUMO→HOMO (93)	1.94	2.06	4.52
3a	1.119	LUMO←HOMO (96)	2.98	3.00	1.158	LUMO→HOMO (97)	2.34	2.45	5.22
3b	1.259	LUMO←HOMO (93)	2.90	2.88	1.257	LUMO→HOMO (95)	2.27	2.39	5.21
3c	1.299	LUMO←HOMO (92)	2.92	2.90	1.238	LUMO→HOMO (97)	2.31	2.10	5.06
3d	1.816	LUMO←HOMO (79)	2.69	2.56	1.763	LUMO→HOMO (90)	2.09	1.99	4.55

[a] Calculated by TD-DFT at level PCM($CHCl_3$)/CAM-B3LYP/6-311+G(2d,p)//PCM($CHCl_3$)/CAM-B3LYP/6-31G(d), corresponding to the $S_1 \leftarrow S_0$ transition (absorption) and $S_1 \rightarrow S_0$ transition (emission). [b] Oscillator strength. [c] Percentage contribution approximated by 2 x $(c_i)^2$ x100%. [d] Calculated (calc.) and experimental (exp.) energies. [e] HOMO–LUMO energy band gap.

MALDI-TOF mass spectra were obtained on a Bruker Autoflex II TOF/TOF spectrometer using dihidroxibenzoic acid (DHB) as the matrix. Samples, co-crystallized with the matrix on the probe, were ionized with a nitrogen laser pulse (337 nm) and accelerated under 20 kV with time-delayed extraction before entering the time-of-flight mass spectrometer. Matrix (10 mg/mL) and sample (1 mg/mL) were separately dissolved in methanol and mixed in a matrix/sample ratio ranging from 100:1 to 50:1. Typically, a 5 µL mixture of matrix and sample was applied to a MALDI-TOF MS probe and air-dried. MALDITOF MS in positive reflector mode was used for all samples. External calibration was performed by using Peptide Calibration Standard II (covered mass range: 700–3200 Da) from Care (Bruker). The applied peak (m/z determination) detection method was the threshold centroid at 50% height of the peak maximum.

UV-Vis spectra were recorded on a Varian Cary model 5000 UV-Vis-NIR spectrophotometer using standard quartz cells of 1 cm width and solvents of spectroscopic grade. Emission spectra were recorded on a FluoTime 300 spectrometer from PicoQuant equipped with a 300 W ozone-free Xe lamp (250–900 nm), a 10 W Xe Flash-lamp (250–900 nm, pulse width < 10ms) with repetition rates of 0.1–300 Hz, an excitation monochromator (Czerny–Turner 2.7 nm mm-1 dispersion, 1200 grooves per mm, blazed at 300 nm), diode lasers (pulse width < 80 ps) operated by a computer-controlled laser driver PDL-820 (repetition rate up to 80 MHz, burst mode for slow and weak decays), two emission monochromators (Czerny–Turner, selectable gratings blazed at 500 nm with 2.7 nm mm^{-1} dispersion and 1200 grooves per mm, or blazed at 1250 nm with 5.4 nm mm^{-1} dispersion and 600 grooves per mm), Glan–Thompson polarizers for excitation (Xe-lamps) and emission, a Peltierthermostatized sample holder from Quantum Northwest (40°C to 105°C), and two detectors, namely a PMA Hybrid 40 (transit time spread FWHM < 120 ps, 300–720 nm) and a R5509- 42 NIR-photomultiplier tube (transit time spread FWHM 1.5 ns, 300–1400 nm) with external cooling (80 °C) from Hamamatsu.

General procedure for derivatives 2a, 2c and 2d: A mixture of 2-(3,5-bis(trifluoromethyl)phenyl)-4,7-dibromo-2*H*-benzo[*d*][1,2,3]triazole (**4**) (0.200 g, 0.41 mmol), the alkenyl derivative (**5**), $Pd(OAc)_2$ (0.9 mg, 0.0041 mmol), NaOAc (0.168 g, 2.05 mmol), *n*-Bu_4NBr (0.0258 g, 0.082 mmol) and DMF (3 mL) was heated at 100°C with efficient stirring for 24h. The fluorescent solution was poured into water. The precipitate was filtered, washed with water, dissolved in dichloromethane and dried over anhydrous $MgSO_4$. After the filtration, the solvent was removed under reduced pressure and the residue was purified by column chromatography on silica gel, obtaining pure products **2a**, **2c** or **2d**.

2-(3,5-bis(trifluoromethyl)-4,7-di((*E*)-styryl-2*H*-benzo[*d*][1,2,3]triazole (2a): From styrene (**5a**) (0.085 g, 0.82 mmol), a yellow solid was obtained (0.147 g, 70%) by chromatography eluting with hexane/ethyl acetate 50:1. m.p: 278-280 °C. ^{1}H-NMR ($CDCl_3$, ppm): 8.98 (s, 2H, *o*-N-Ph), 8.06 (d, 2H, $H_{CH=CH}$, *J* = 16.3 Hz), 8.01 (s,1H, *p*-N-Ph), 7.69 (d, 4H, *o*-Ph, *J* = 7.4 Hz), 7.53 (s, 2H, H_{BTz}), 7.51 (d, 2H, $H_{CH=CH}$, *J* = 16.3 Hz), 7.45 (t, 4H, *m*-Ph, *J* = 7.8 Hz), 7.34 (t, 2H, *p*-Ph, *J* = 7.3 Hz). ^{13}C-NMR ($CDCl_3$, ppm): 203.4, 144.3, 141.4, 137.6, 133.5, 132.8, 128.6, 127.9, 127.8, 127.2, 126.7, 124.2, 120.7. MS calculated for ($C_{30}H_{19}F_6N_3$) 535.15, found 535.11 g/mol.

2-(3,5-bis(trifluoromethyl)-4,7-bis((*E*))-3,4,5-trimethoxystyryl)-2*H*-benzo[*d*][1,2,3]triazole (2c): From 1,2,3-trimethoxy-5-vinylbenzene (**5c**) (0.161 g, 0.84 mmol), an orange solid was obtained (0.260 g, 86%) by chromatography eluting with hexane/ethyl acetate 5:1. m.p: 228-230 °C. ^{1}H-NMR ($CDCl_3$, ppm): 8.98 (s, 2H, *o*-N-Ph), 8.03 (d, 2H, $H_{CH=CH}$, *J* = 16.5 Hz), 8.02 (s,1H, *p*-N-Ph), 7.51 (s, 2H, H_{BTz}), 7.38 (d, 2H, $H_{CH=CH}$, *J* = 16.5 Hz), 6.90 (s, 4H, H-Ph), 3.99 (s, 12H, *m*-OCH_3), 3.97 (s, 6H, *p*-OCH_3). ^{13}C-NMR ($CDCl_3$, ppm): 153.6, 144.4, 141.1, 138.6, 133.8, 133.5, 133.1, 127.7, 127.2, 123.9, 122.2, 120.7, 107.3, 104.1, 61.0, 56.2. MS calculated for ($C_{36}H_{31}F_6N_3O_6$) 716.21, found 716.13 g/mol.

4,4'-((1*E*,1'*E*)-(2-(3,5-bis(trifluoromethyl)phenyl)-2*H*-benzo[*d*][1,2,3]triazole-4,7-diyl)bis(ethene-2,1-diyl))bis(*N*,*N*-diphenylaniline) (2d): From *N*,*N*-diphenyl-4-vinylaniline (**5d**) (0.220 g, 0.82 mmol), a deep red solid was obtained (0.255 g, 73%) by chromatography eluting with hexane/ethyl acetate 50:1. m.p: 138-140 °C. ^{1}H-NMR ($CDCl_3$, ppm): 8.96 (s, 2H, *o*-N-Ph), 8.00 (s, 1H, *p*-N-Ph), 7.99 (d, 2H, $H_{CH=CH}$, *J* = 16.0 Hz), 7.55 (d, 4H, H-Ph, *J* = 8.6 Hz), 7.47 (s, 2H, H_{BTz}), 7.39 (d, 2H, $H_{CH=CH}$, *J* = 16.0 Hz), 7.33-7.29 (m, 8H, H-Ph), 7.18 (d, 8H, H-Ph, *J* = 8.5 Hz), 7.13 (d, 4H, H-Ph, *J* = 8.6 Hz), 7.09 (t, 4H, H-Ph, *J* = 7.4 Hz). ^{13}C-NMR ($CDCl_3$, ppm): 147.9, 147.5, 144.4, 141.2, 133.3, 133.1, 132.8, 131.5, 131.2, 129.4, 127.8, 127.7, 126.6, 125.1, 124.7, 123.3, 122.7, 120.5. MS calculated for ($C_{54}H_{37}F_6N_5$) 869.30, found 869.15 g/mol.

4,7-bis((*E*)-2-benzo[b]thiophen-7-yl)vinyl)-2-(3,5-bis(trifluoromethyl)phenyl)-2*H*-benzo[*d*][1,2,3]triazole (2b): A mixture of 4,7-bis(benzo[*b*]thiophen-7-ylethynyl)-2-(3,5-bis(trifluoromethyl)phenyl)-2*H*-benzo[*d*][1,2,3]-triazole (**1b**) (0.156 g, 0.24 mmol), $HSiEt_3$ (0.14 g, 0.0012 mmol), $PdCl_2$ (dppf) (0.008 g, 0.001 mmol), dppf (0.017 g, 0.00003 mmol), $CuSO_4$ (0.035 g, 0.0001 mmol), toluene/H_2O (5 mL / 1 mL) was heated at 120°C for 12 hours. The end of the reaction was detected by TLC. Finally, an orange solid was obtained (0.064 g, 41%) by chromatography eluting with hexane/ethyl acetate 50:1. m.p: 200-202 °C. ^{1}H-NMR ($CDCl_3$, ppm): 9.2 (s, 2H, *o*-N-Ph), 8.67 (d, 2H, $H_{CH=CH}$, *J* = 16.4 Hz), 8.03 (s, 1H, *p*-N-Ph), 7.83 (d, 2H, $H_{thiophene}$, *J* = 7.2 Hz), 7.78 (d, 2H, $H_{thiophene}$, *J* = 7.6 Hz), 7.63 (s, 2H, H_{BTz}), 7.61 (d, 2H, $H_{CH=CH}$, *J* = 16.4 Hz), 7.57 (d, 2H, H-Ar, *J* = 5.2 Hz), 7.5 (t, 2H, H-Ar, *J* = 4.0 Hz), 7.46 (d, 2H, H-Ar, *J* = 5.5 Hz). ^{13}C-NMR ($CDCl_3$, ppm): 144.2, 141.0, 140.4, 139.4, 139.3, 133.4, 132.0, 131.9, 128.3, 128.0, 126.0, 126.0, 124.8, 124.0, 123.4, 120.8, 120.4, 114.1. MS calculated for ($C_{34}H_{19}F_6N_3S_2$) 647.10, found 647.19 g/mol.

4-(benzo[*b*]thiophen-4-ylethynyl)-7-(benzo[*b*]thiophen-7-ylethynyl)benzo[*c*][1,2,5]thiadiazole (3b): A mixture of 4,7-dibromobenzo[*c*][1,2,5]thiadiazole (0.100 g, 0.34 mmol), 7-ethynylbenzo[*b*]thiophene (**6b**) (0.108 g, 0.68 mmol), DBU (0.104 g, 0.68 mmol), CuI (0.003 g, 0.01 mmol) and Pd-EncatTM TPP30 (0.031 g, 0.012 mmol) was charged under argon to a dried microwave vessel. CH_3CN (1 mL) was added. The vessel was closed and irradiated at 130°C for 20 min. The crude reaction product was purified by chromatography, eluting with hexane/ethyl acetate 9:1 and a brown solid was obtained (0.111 g, 72%). m.p: 240-242 °C. ^{1}H-NMR ($CDCl_3$, ppm): 7.93 (s, 2H, H_{BTD}), 7.89 (d, *J* = 7.4 Hz, 2H, H-Ar), 7.70 (d, *J* = 7.4 Hz, 2H, H-Ar), 7.59 (d, *J* = 5.4 Hz, 2H, $H2_{thiophene}$), 7.45 (t, *J* = 7.4 Hz, 2H, H-Ar), 7.44 (d, *J* = 5.4 Hz, 2H, $H3_{thiophene}$). ^{13}C-NMR ($CDCl_3$, ppm): 154.4, 142.8, 139.6, 132.5, 128.0, 127.3, 124.6, 124.4, 124.3, 117.2, 117.0, 95.1, 89.9. MS calculated for ($C_{26}H_{12}N_2S_3$) 448.02, found 448.44 g/mol.

Two-photon microscopy: Briefly, the two-photon absorption cross sections (σ) were determined following a standard procedure,[36] using concentrations for all compounds under 10^{-5} M to avoid aggregation phenomena. The laser power regime was delimited to ensure a lineal correlation between the logarithm of the fluorescence intensity and the logarithm of the excitation power, attending to the two-photon excitation fluorescence measurements. As reference, Rhodamine B (10^{-5} M in methanol) was employed, assuming that regardless if two-photon or single-photon are employed to excite the molecule, the fluorescence quantum yield is the same. The fluorescence properties of the compounds were investigated using an inverted Leica SP5 MP confocal microscope with a MaiTai Ti-Sapphire HP laser (Spectra-Physics, Inc.) tunable between 690 and 1040nm. The spectra were recorded using a 10x Plan APO objective (NA 0.4) focused at the air/liquid boundary, allowing the simultaneous detection of both background and sample fluorescence. Emission spectra were measured using a dynamic 30 nm wide emission detection window moving in 20 steps between 380 and 700 nm.

Considering regions of interest (ROIs), emission and excitation spectra data were registered using Leica LAS AF software.

DFT calculations: All calculations were accomplished using Gaussian 16A03 package.[44] The effect of the solvent was considered by including the polarizable continuum model (PCM) and specifying chloroform as solvent. Employing the Coulomb Attenuated CAM-B3LYP functional[40] with the 6-31G(d) basis set,[41] both ground (S_0) and excited (S_1) state geometrical parameters were optimized by density functional theory (DFT). The nature of the minima was confirmed by the absence of a negative frequency in analytical Hessian calculations. Absorption and emission energies were computed by using the linear-response (LR) approach, considering the time-dependent density functional theory (TD-DFT) and employing in this case 6-311+G(2d,p) basis set for the first ten excited states. Natural transition orbitals (NTOs) were calculated to describe the physical feature of holes and electrons in the excited states.[43] The TPA cross-sections were estimated at the TD-CAM-B3LYP/6-31G level on the minimal ground state geometries using Dalton 2018 with the default parameters.[45,46] OP and TP absorption spectra were simulated with Gaussum.[47] For OP spectra, the spectral window was delimited from 200 nm until 800 nm, while for TP spectra, this window was set from 300 nm until 1000 nm. Gaussian function was used to give shape to the spectra, with a set FWHM of 1000 cm^{-1} and sigma of 0.2.

Acknowledgements

This work was supported by the Spanish Ministerio de Economía, Industria y Competitividad (CTQ2016-75870-P) and by Junta de Comunidades de Castilla-La Mancha and FEDER (SBPLY/17/180501/000189). Instituto de Salud Carlos III (ISCIII; RETIC ARADYAL RD16/0006/0012), Consejería de Salud, Junta de Andalucía (PI0250-2016) and FEDER founds. C.B-M. holds a FPU grant of MECD (FPU16/02516) and B.D. holds a FPU grant of MECD (FPU16/05099). We gratefully acknowledge the computer resources provided by the SCBI (Supercomputing and Bioinformatics Center) of the University of Malaga and High Performance Computing Service of the University of Castilla-La Mancha.

Keywords: Benzotriazole • Two-photon absorption • Dyes • Fluorescence •

[1] R. Li, J. Byun, W. Huang, C. Ayed, L. Wang, K. A. I. Zhang, *ACS Catal.* **2018**, *8*, 4735–4750.

[2] W. Qin, P. Zhang, H. Li, J. W. Y. Lam, Y. Cai, R. T. K. Kwok, J. Qian, W. Zheng, B. Z. Tang, *Chem. Sci.* **2018**, *9*, 2705–2710.

[3] I. Martynov, A. V Akkuratov, S. Luchkin, S. Tsarev, S. D. Babenko, V. G. Petrov, K. J. Stevenson, P. A. Troshin, *ACS Appl. Mater. Interfaces* **2019**, *11*, 21741−21748.

[4] R. Martín, P. Prieto, J. R. Carrillo, I. Torres, C. A. Strassert, K. Soloviova, A. M. Rodríguez, L. Sánchez, Á. Díaz-Ortiz, *Dye. Pigment.* **2018**, *151*, 327–334.

[5] I. Torres, J. R. Carrillo, A. Díaz-Ortiz, R. Martín, M. V. Gómez, L. Stegemann, C. A. Strassert, J. Orduna, J. Buendía, E. E. Greciano, et al., *RSC Adv.* **2016**, *6*, 36544–36553.

[6] I. Torres, A. Díaz-Ortiz, L. Sánchez, J. Orduna, M. J. Blesa, J. R. Carrillo, P. Prieto, *Dye. Pigment.* **2017**, *142*, 212–225.

[7] L. Hamenu, A. Madzvamuse, L. Mohammed, Y. M. Lee, J. M. Ko, C. Y. Bon, S. J. Kim, W. Il Cho, Y. G. Baek, J. Park, *J. Ind. Eng. Chem.* **2017**, *53*, 241–246.

[8] W. Li, L. Yan, H. Zhou, W. You, *Chem. Mater.* **2015**, *27*, 6470–6476.

[9] B. Fan, K. Zhang, X. F. Jiang, L. Ying, F. Huang, Y. Cao, *Adv. Mater.* **2017**, *29*, DOI 10.1002/adma.201606396.

[10] Y. Yang, B. Jia, J. Wang, T. K. Lau, X. Lu, X. Zhan, X. Chen, *Polymer (Guildf).* **2018**, *139*, 123–129.

[11] M. K. Pola, K. M. Boopathi, H. Padhy, P. Raghunath, A. Singh, M. C. Lin, C. W. Chu, H. C. Lin, *Dye. Pigment.* **2017**, *139*, 349–360.

[12] I. Torres-Moya, I. Arrechea-Marcos, C. Tardío, J. R. Carrillo, Á. Díaz-Ortiz, J. T. López Navarrete, M. C. Ruiz Delgado, P. Prieto, R. P. Ortiz, *RSC Adv.* **2018**, *8*, 21879–21888.

[13] I. Torres-Moya, B. Saikia, P. Prieto, J. R. Carrillo, J. W. Steed, *CrystEngComm* **2019**, *21*, 2135–2143.

[14] R. Vázquez-Guilló, M. J. Martínez-Tomé, Z. Kahveci, I. Torres, A. Falco, R. Mallavia, R. C. Mateo, *Polymers (Basel).* **2018**, *10*, 938.

[15] M. Göppert-Mayer, *Ann. Phys.* **1931**, *401*, 273–294.

[16] J. H. Strickler, W. W. Webb, in *CAN-AM East. '90* (Eds.: R.L. Antos, A.J. Krisiloff), International Society For Optics And Photonics, **2012**, pp. 107–118.

[17] D. A. Parthenopoulos, P. M. Rentzepis, *Science (80-.).* **1989**, *245*, 843–845.

[18] J. H. Strickler, W. W. Webb, *Opt. Lett.* **1991**, *16*, 1780.

[19] W. Denk, J. H. Strickler, W. W. Webb, *Science (80-.).* **1990**, *248*, 73–76.

[20] O. Mongin, L. Porrès, M. Charlot, C. Katan, M. Blanchard-Desce, *Chem. - A Eur. J.* **2007**, *13*, 1481–1498.

[21] S. J. Chung, S. Zheng, T. Odani, L. Beverina, J. Fu, L. A. Padilha, A. Biesso, J. M. Hales, X. Zhan, K. Schmidt, et al., *J. Am. Chem. Soc.* **2006**, *128*, 14444–14445.

[22] M. Albota, S. E. Hess, W. W. Webb, C. Xu, D. Bel-jonne, J. Brédas, J. Fu, A. A. Heikal, M. Rumi, X. Wu, et al., *Science (80-.).* **1998**, *281*, 1653–1656.

[23] L. Beverina, J. Fu, A. Leclercq, E. Zojer, P. Pacher, S. Barlow, E. W. Van Stryland, D. J. Hagan, J. L. Brédas, S. R. Marder, *J. Am. Chem. Soc.* **2005**, *127*, 7282–7283.

[24] O. Varnavski, X. Yan, O. Mongin, M. Blanchard-Desce, T. Goodson, *J. Phys. Chem. C* **2007**, *111*, 149–162.

[25] M. Pawlicki, H. A. Collins, R. G. Denning, H. L. Anderson, *Angew. Chem. Int. Ed. Engl.* **2009**, *48*, 3244–66.

[26] S. I. Kato, T. Matsumoto, T. Ishi-I, T. Thiemann, M. Shigeiwa, H. Gorohmaru, S. Maeda, Y. Yamashita, S. Mataka, *Chem. Commun.* **2004**, *10*, 2342–2343.

[27] S. I. Kato, T. Matsumoto, M. Shigeiwa, H. Gorohmaru, S. Maeda, T. Ishi-i, S. Mataka, *Chem. - A Eur. J.* **2006**, *12*, 2303–2317.

[28] Z. Di Yang, J. K. Feng, A. M. Ren, *J. Mol. Struct. THEOCHEM* **2008**, *848*, 24–33.

[29] M. N. K. Prasad Bolisetty, C. T. Li, K. R. Thomas Justin, G. B. Bodedla, K. C. Ho, *Tetrahedron* **2015**, *71*, 4203–4212.

[30] C. A. Faler, M. M. Joullié, *Org. Lett.* **2007**, *9*, 1987–1990.

[31] F. Luo, C. Pan, W. Wang, Z. Ye, J. Cheng, *Tetrahedron* **2010**, *66*, 1399–1403.

[32] R. P. Haugland, M. T. Z. Spence, I. D. Johnson, A. Basey, *The Handbook: A Guide to Fluorescent Probes and Labeling Technologies.*, **2005**.
[33] E. Lippert, *Zeitschrift für Naturforsch. A* **1955**, *10*, 541–545.
[34] N. Mataga, Y. Kaifu, M. Koizumi, *Bull. Chem. Soc. Jpn.* **1955**, *28*, 690–691.
[35] N. Mataga, Y. Kaifu, M. Koizumi, *Bull. Chem. Soc. Jpn.* **1956**, *29*, 465–470.
[36] F. Terenziani, C. Katan, E. Badaeva, S. Tretiak, M. Blanchara-Desce, *Adv. Mater.* **2008**, *20*, 4641–4678.
[37] M. Drobizhev, F. Meng, A. Rebane, Y. Stepanenko, E. Nickel, C. W. Spangler, *J. Phys. Chem. B* **2006**, *110*, 9802–9814.
[38] P. Remón, S. M. Li, M. Grotli, U. Pischel, J. Andréasson, *Chem. Commun.* **2016**, *52*, 4659–4662.
[39] Á. M. Marín, J. P. Telo, D. Collado, F. Nájera, E. Pérez-Inestrosa, U. Pischel, *Chem. - A Eur. J.* **2018**, *24*, 2929–2935.
[40] T. Yanai, D. P. Tew, N. C. Handy, *Chem. Phys. Lett.* **2004**, *393*, 51–57.
[41] V. A. Rassolov, J. A. Pople, M. A. Ratner, T. L. Windus, *J. Chem. Phys.* **1998**, *109*, 1223–1229.
[42] J. Tomasi, B. Mennucci, R. Cammi, *Chem. Rev.* **2005**, *105*, 2999–3094.
[43] R. L. Martin, *J. Chem. Phys.* **2003**, *118*, 4775–4777.
[44] M. J. Frisch, G. W. Trucks, H. B. Schlegel, G. E. Scuseria, M. A. Robb, J. R. Cheeseman, G. Scalmani, V. Barone, G. A. Petersson, H. Nakatsuji, et al., **2016**. Gaussian 16 (Revision A03)
[45] K. Aidas, C. Angeli, K. L. Bak, V. Bakken, R. Bast, L. Boman, O. Christiansen, R. Cimiraglia, S. Coriani, P. Dahle, et al., *Wiley Interdiscip. Rev. Comput. Mol. Sci.* **2014**, *4*, 269–284.
[46] Dalton a molecular electronic structure program, Release v2018.2 (2018), see http://daltonprogram.org (accessed 30/09/2019)
[47] N. M. O'Boyle, A. L. Tenderholt, K. M. Langner, *J. Comput. Chem.* **2008**, *29*, 839–845.

Entry for the Table of Contents

FULL PAPER

A newfangled two-photon chromophore scaffold: a promising electron-withdrawing improved benzotriazoles derivatives with exceptional photophysical properties have been prepared. The study of their structure-properties relationship allows to afford high brightness and great cross-sections.

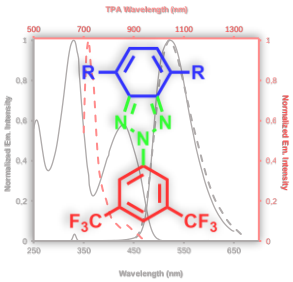

Iván Torres-Moya, Carlos Benitez-Martin, Beatriz Donoso, Carlos Tardío, Raúl Martín, José R. Carrillo, Ángel Díaz-Ortiz, Francisco Najera, Pilar Prieto,* and Ezequiel Perez-Inestrosa**

Page No. – Page No.

Extended Alkenyl and Alkynyl Benzotriazoles with Enhanced Two-Photon Absorption Properties as a Promising Alternative to Benzothiadiazoles